Preprints of the 19th World Congress
The International Federation of Automatic Control
Cape Town, South Africa. August 24-29, 2014

Modeling and Parameter Identification for CO_2 Post-Combustion Capture by Amines Supported on Solid Sorbents ⋆

L. Bisone * **S. Bittanti** (IFAC fellow) ** **S. Canevese** ***
A. De Marco * **S. Garatti** ** **M. Notaro** *** **V. Prandoni** ***

* *Consultant, 20134, Milan, Italy (e-mail: lbis1@inwind.it, antoniodemarco65@gmail.com)*
** *Dipartimento di Elettronica, Informazione e Bioingegneria, Politecnico di Milano, Piazza Leonardo da Vinci 32, 20133 Milan, Italy (e-mail: {sergio.bittanti,simone.garatti}@polimi.it)*
*** *RSE S.p.A., 20134, Milan, Italy (e-mail: {canevese, maurizio.notaro,valter.prandoni}@rse-web.it)*

Abstract: A recently proposed technique for post-combustion CO_2 capture in fixed-bed reactors is based on an absorption procedure carried out by amine supported on pelleted solid substrates. This procedure is one of the most promising technologies, in particular because it is less energy intensive than absorption by amines in aqueous solutions. With reference to a laboratory diabatic tubular reactor, a dynamic lumped-parameter model is worked out with physical reasoning. The main two unknown parameters in the model are the CO_2 absorption and desorption coefficients. These two parameters are identified by a two-step white-box technique. Identification is performed thanks to real data collected in laboratory experiments.

Keywords: Solid sorbent, supported amine, CO_2 capture, process modeling, online parameter identification.

1. INTRODUCTION

Even if the process based on chemical absorption by aqueous alkanolamine solvents, Ciferno et al. (2007), is believed the most viable near-term technology for post-combustion CO_2 capture from power plants flue gases, it has not been demonstrated on full-scale plants yet and has a number of drawbacks in treating flue gases, such as corrosion, foam formation and amine degradation due to oxidation mechanisms. Moreover, it is highly energy intensive, especially in the sorbent regeneration stage. Therefore, many research efforts have been devoted to conceive different kinds of technologies. Several *solid* sorbents, in particular, with or without amines, have been tested (Krutka and Sjostrom (2011)). Solid sorbents can achieve both higher gas absorption rate and larger absorption capacity than the solvent absorption technology. Moreover, they have both lower heat capacity and lower regeneration temperature and thus allow an energy consumption reduction.

In this work, we focus on an innovative process based on chemical absorption by diethanolamine (DEA) supported on highly porous solid alumina pellets (Notaro and Pinacci (2007), Notaro et al. (2012)). The proposed absorbent is low cost, has high CO_2 selectivity, high absorption capacity and low specific heat (Notaro (2011)). Moreover, the use of amine as reagent anchored on the solid surface, and not dissolved in water, provides greater amine stability to the oxidative degradation and avoids corrosion problems.

The configuration of the considered CO_2 capture process (Bittanti et al. (2012)) is based on a fixed-bed absorption/desorption diabatic unit operating in a TSA (Temperature Swing Absorption) mode or in a combined TSA/PSA (Pressure Swing Absorption) mode. This unit is a finned tube heat exchanger operating alternatively as adsorber or desorber (cooled in absorption and heated in desorption) with the sorbent loaded into the free space between the fins. The fixed-bed solution needs a small pressure drop ($5000Pa$) for the application in power stations, so a solid sorbent in pellets form of suitable size is employed.

The best prepared sorbents (DEA on 3 mm alumina spheres) showed a "net CO_2 capture" of 50 mg CO_2/g of sorbent (5% wt) and a "useful time" of 40 minutes at 40 °C with a sorbent load of 650 g and a gas flow rate of 300 Nl/h (gas composition: 10% CO_2, 3% O_2, 10% H_2O in N_2). The sorbent is completely regenerated by heating the absorption unit up to 85 °C, while depressurizing it and stripping it with a low steam flow.

As compared to a conventional CO_2 capture process based on a 30 wt% monoethanolamine (MEA) aqueous solution, the proposed process allows to save 35% of the heat required for the sorbent regeneration, so it could be applied

⋆ This work has been financed by the Research Fund for the Italian Electrical System under the Contract Agreement between RSE S.p.A. and the Ministry of Economic Development - General Directorate for Nuclear Energy, Renewable Energy and Energy Efficiency in compliance with the Decree of March 8, 2006. The support by the MIUR national project "Identification and adaptive control of industrial systems" and by CNR - IEIIT is also gratefully acknowledged.

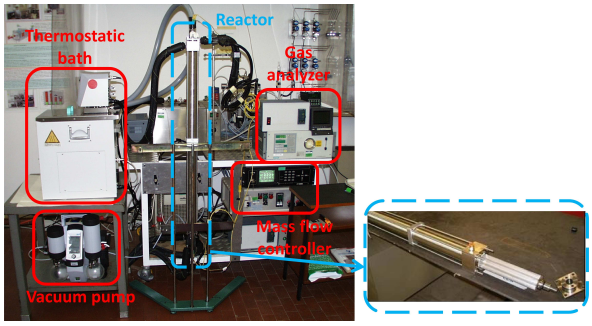

Fig. 1. RSE laboratory-scale plant and a detail of the reactor for CO_2 absorption/desorption

on a coal thermal power plant with a 3% energy saving with respect to the MEA aqueous solution process (and with 90% efficiency).

The paper is organized as follows. Section 2 describes a dynamic model of the absorption/desorption process, based on conservation equations in one/two-dimensional geometry and a rather detailed kinetic-chemical description. In Sections 3-4, identification of the main unknown parameters in the model is discussed, by resorting to a new method introduced in Garatti and Bittanti (2013).

This research activity is based on experimental data (Notaro (2011)) collected on a laboratory-scale plant (described in Section 3 and shown in Fig. 1), located at RSE "Processes and catalytic materials" laboratory in Piacenza (Italy).

2. PROCESS DESCRIPTION AND REACTOR MODEL

The fixed-bed reactor taken as a reference here (Fig. 1) is conceived as a heat exchanger composed of an inner extruded aluminium finned tube, with outer fins extending radially all along its length, and an outer 316 stainless steel tube shell. The sorbent is made up of highly porous approximately spherical pellets (radius $R_0 = 1.5 \cdot 10^{-3}$ m and mass density $\rho_s = 680$ kg/m^3) with 36% wt. DEA contents. The sorbent fills the space between the tube and the shell; a porous metallic disk at the bottom of the reactor supports the pellets. The reactor is 1 m long, with inner and outer radii $R_{in} = 0.012$ m and $R_{ex} = 0.0225$ m respectively and a cross sectional area $A = 0.9695 \cdot 10^{-3}$ m^2; it can operate with about 1 kg of sorbent load (0.647 kg were employed in the described tests). A thermal fluid (diathermal oil), supplied by an external refrigerating and heating circulator, flows into a coil inside the tube, to avoid direct contact with the sorbent, and it heats, or cools, by conduction the sorbent in the cavities between fins. The conductive heat exchange with the sorbent is improved by an external jacket where the thermal fluid flow rate from the finned tube outlet can be conveyed (*i.e.* in an ideally series configuration).

The temperature of the fixed-bed sorbent is measured by three type K thermocouples placed respectively at the beginning (point A), in the middle and at the end (point B) of the sorbent bed. The inlet and the outlet reactor gas composition are measured by continuous analyzers specifically designed for CO_2 (Siemens, ULTRAMAT 5E) and recorded by a data logger with 1 Hz sample rate. A vacuum pump depressurizes the reactor during the regeneration carried out as a combination of TSA and PSA modes.

In our experiments, CO_2, N_2 and H_2O vapor are used as gas feed for parameter identification (Section 3). In the typical composition of flue gases in conventional power stations, there are also O_2, SO_2 and NO: these have not been included in the feed gas mixture, because they would have altered the DEA, by oxidation or by irreversible absorption.

Fig. 2 shows a scheme of the reactor, with the bulk gas flow along the axial coordinate z and with the pellet spheres inside. The overall reaction on the sorbent surface is

$$\underbrace{2R_2NH}_{DEA} + CO_2 \underset{des}{\overset{abs}{\rightleftarrows}} \underbrace{R_2NH_2^+ + R_2NCO_2^-}_{DEA^*}. \qquad (1)$$

In the absorption phase, the feedgas mixture reaches the sphere outer surface crossing its limit layer; then, it flows inside the sphere, into its pores, and CO_2 reacts with the anchored DEA, by the absorption reaction; in the desorption phase, the reverse reaction occurs, CO_2 is released and leaves the pellet to reach the bulk flow.

For modelling purposes, a standard finite-volume approach is adopted here, as in Bittanti et al. (2010) and De Marco et al. (2010): we refer to those papers for a detailed description of the equations. In few words, the reactor length L is divided into N_c strips (see Fig. 2), in each of which the bulk gas behaviour is described by lumped-parameter mass, energy and momentum Conservation Equations (CEs). The process variables in the generic k-th strip, Δz_k long, between z_k and z_{k+1}, are defined by their average value along z between z_k and z_{k+1}. For simplicity, all strips are assumed as identical: $\Delta z_k = \Delta z = L/N_c$, $\forall k = 0, \ldots, N_c - 1$. Similarly, an average equivalent spherical pellet, of radius R_0, is divided into N_r spherical shell volumes and lumped-parameter mass and momentum CEs are considered in each i-th shell, $i = 0, \ldots, N_r - 1$[1]. Here, all shells are assumed to have the same volume $V_g = 4\pi {R_0}^3/(3N_r)$. In the CEs for the bulk region, the "effect" of a single pellet is multiplied by the average number of pellets in a strip, i.e. $N_p \Delta z/L$, with N_p the total number of pellets in the reactor. Energy CEs in the sorbent are written with reference to a sorbent average temperature T_k in each strip k, instead of a temperature in each shell for each strip.

The terms included in the CEs and the main simplifying assumptions can be thus summarized (compare also Ruthven (1984), Ruthven et al. (1994) and Santacesaria et al. (1982)):

- *chemical kinetics*:
  - active site CEs (written for $i = 1, \ldots, N_r$, $k = 0, \ldots, N_c - 1$) describe CO_2 absorption and desorption into the pellets (see (2));
- *hydrodynamic equations*:
  - global mass CEs in the pellets (for $i = 1, \ldots, N_r$,

[1] With reference to N_c strips and N_r shells for each strip, the overall non-linear lumped-parameter dynamic model proposed here is of order $N = 2N_c(N_r + 1)$. The simulation results described in the following have been obtained for N_c =20 and N_r=3, so that N=160.

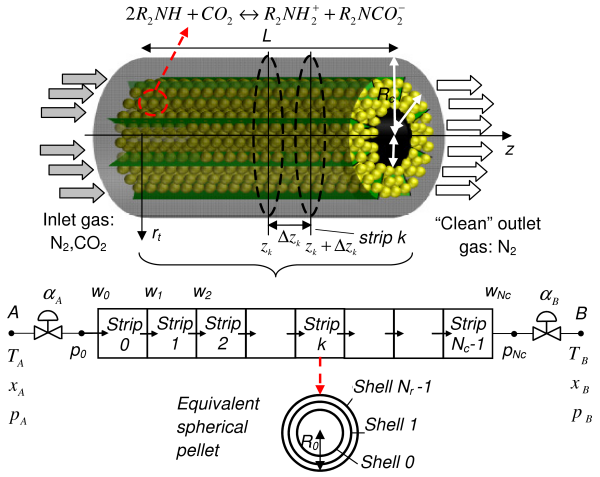

Fig. 2. Top: scheme of the absorption/desorption reactor; bottom: reference structure for the reactor model

$k = 0, \ldots, N_c - 1$) are written in quasi-steady state conditions, with bulk-sorbent boundary flow rate due to absorption from all shells and with no convective flow rate at the sphere centre;
- global mass CEs along the bulk flow (for $k = 0, \ldots, N_c - 1$) adopt the quasi-stationary assumption for p and T, so accumulation is neglected;
- momentum CEs in the bulk region (for $k = 0, \ldots, N_c$) are written in quasi-steady state conditions and include laminar friction only;

- *mass conservation equations*:
  - CO_2 mass CEs in the pellet volume (for $i = 0, \ldots, N_r - 1$, $k = 0, \ldots, N_c - 1$) account for CO_2 accumulation, absorption/desorption, radial diffusion to/from the adjacent shells, radial convection to/from the adjacent shells;
  - CO_2 mass CEs in the bulk volume (for $k = 0, \ldots, N_c - 1$) include CO_2 accumulation, convective and diffusive mass exchange with the pellet surface, bulk axial diffusion to/from the adjacent strips, bulk axial convection to/from the adjacent strips;
- *energy conservation equations*:
  - energy CEs in the sorbent volume (for $k = 0, \ldots, N_c - 1$) include energy accumulation, conduction in the reactor axial direction to/from the adjacent strips, absorption/desorption reaction heat, heat exchange between the pellets and the bulk gas, heat exchange between the pellets and the exchanger metal surface;
  - energy CEs in the bulk volume (for $k = 0, \ldots, N_c - 1$) describe heat exchange between the pellets and the bulk gas, energy axial transport to/from the adjacent strips (by bulk flow rate), energy axial conduction to/from the adjacent strips; accumulation is neglected in the bulk gas.

Boundary conditions for pressure p and/or bulk molar flow rate w, and also for temperature T, at the reactor inlet and/or outlet are set by two valves A and B (see Fig. 2).

As for chemical kinetics in particular, CO_2 absorption and desorption into the sorbent, in shell i in strip k, can be described, according to the Langmuir theory (Froment and Bischoff (1990)), by

$$\begin{aligned}&\varphi\dot{\theta}_{k,i}(t) = k_{abs}\left(T_k(t)\right)\cdot\left(1-\theta_{k,i}(t)\right)\cdot C_{k,i}(t) + \\ &-k_{des}\left(T_k(t)\right)\cdot C_{ref}\cdot\theta_{k,i}(t), C_{ref} = p_{ref}/(RT_{ref}),\end{aligned} \quad (2)$$

where $\theta_{k,i}$ is the area fraction occupied by CO_2 molecules tied to the DEA on the porous medium surface, $C_{k,i}$ is the CO_2 molar concentration, in the gas phase, in the porous medium, T_k is the sorbent temperature in strip k. φ represents the *kmol* of DEA sites which can be occupied by CO_2 in 1 m^2 of active surface. The standard conditions are assumed as the reference for pressure and temperature: $p_{ref} = 101000$ Pa, $T_{ref} = 298$ K. k_{abs} and k_{des} are, respectively, the absorption and desorption kinetic parameters in the reaction between CO_2 and DEA free sites; they are the main uncertain parameters in the model. Note that they depend on the temperature T in the porous medium, while their dependence on pressure is negligible (Froment and Bischoff (1990)). Their identification is addressed in Section 3.

3. MODEL KINETIC PARAMETERS IDENTIFICATION VIA BENCH EXPERIMENTS

In order to identify the kinetic parameters of the described model, twelve *ad hoc* dynamic tests have been carried out on the test rig. More precisely, starting from completely regenerated sorbent, absorption has been carried out by feeding the reactor with N_2, steam (10% molar fraction) and CO_2 mixtures with fixed CO_2 concentrations, setting the inlet gas flow rates by means of the mass-flow controllers ($w_f = 219$ Nl/h was the total feedgas flow rate, with $SV = w_f/M_s = 0.45$ Nl/(h·g) space velocity), and keeping the reactor temperature constant and uniform by using the external circulator. Three different inlet mixtures (with CO_2 molar fraction equal to 0.05, 0.10 and 0.25 respectively) and four temperatures (25 °C, 40 °C, 60 °C and 85 °C) have been considered. In each test, the CO_2 molar fraction at the reactor outlet x_{CO_2out} was measured, up to the final steady state of complete sorbent saturation ($\theta = 1$ in (2)); measures of the sorbent temperature at the reactor centre were available as well. The measured x_{CO_2out} allowed computing the amount Γ (kmol) of adsorbed CO_2 in each test. The adopted identification procedure can be summed up as follows.

First, the steady-state results of the tests have been considered: the obtained values for Γ have been employed to evaluate the ratio $\eta := k_{abs}/k_{des}$ and the amount of CO_2, in terms of kmol/m^2, which can be adsorbed at complete saturation, i.e. parameter φ in (2). Parameter φ, namely the amount of active sites per unit sorbent surface, is taken as a constant here, and it is estimated as $\varphi = 1.09 \cdot 10^{-3}\rho_s/(\gamma M_s) = 2.4145 \cdot 10^{-8}$ kmol/m^2, with $\gamma = 43.3 \cdot 10^6$ m^2/m^3 the active surface per unit volume. We notice that keeping the inlet concentration constant yields an increasing Γ as temperature decreases. These steady-state Γ values have also allowed to identify the standard enthalpy variation of reaction (1), as $(\Delta H_r)_0 = -55.4 \cdot 10^6$ J/kmol.

Then, the dynamic results of three of the twelve tests (with inlet CO_2 molar fraction equal to 0.1 and at 40 °C, 60 °C and 85 °C temperature) have been considered, to determine each of the two parameters k_{abs} and k_{des}, as a function of the temperature. More precisely, an optimization procedure has been followed, searching for the minimum

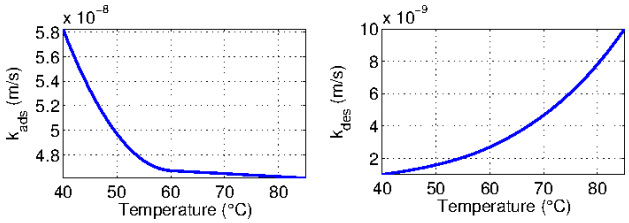

Fig. 3. The identified $k_{abs}(T)$ and $k_{des}(T)$

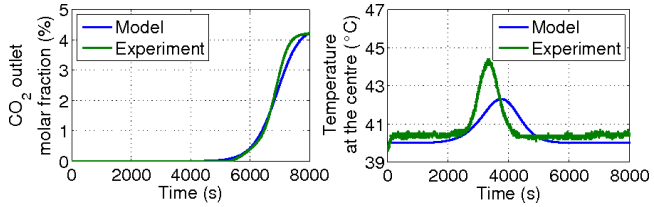

Fig. 4. Model output versus experimental data: CO_2 outlet molar fraction, temperature at the reactor centre

error between the simulated and the measured CO_2 outlet molar fraction in each of the three tests, while ensuring that $k_{abs}(T)$ is decreasing with increasing temperature and $k_{des}(T)$ increasing with increasing temperature. Fig. 3 depicts the thus identified functions $k_{abs}(T)$ and $k_{des}(T)$.

Finally, the model has been validated by comparing transient simulation results to the dynamic results of other tests of the twelve. An example of such comparison is shown in Fig. 4, for a test with 5% inlet CO_2 molar fraction and 40 °C temperature in the absorption phase. The model is able to reproduce the main features of the CO_2 molar fraction transients at the reactor outlet and of the reactor temperature transients, in all working conditions; in particular, increasing and decreasing trends are predicted correctly. Model adherence to the system behaviour, especially as to temperatures, could be increased by further improving parameter tuning. Several parameters in the model, in fact, have been taken from literature data so far, and thus they are subject to uncertainty.

4. ON-LINE IDENTIFICATION: THE TWO-STAGE (TS) APPROACH

As time progresses, the identified model parameters become obsolete, because the reactor for CO_2 absorption/desorption receives constant wear during its operating life. Hence, in principle, the procedure for parameter estimation has to be continuously repeated. On the opposite, we can provide an estimation algorithm able to supply the model parameters whenever a new experiment is performed on the plant, without the intervention of qualified personnel. Moreover, it should be able to generate estimates at low computational cost.

The identification problem belongs to the white-box category, being a realistic model of the plant available except the knowledge of few parameters. These latter are the coefficients a, b, and c of the parabola through which the dependence of k_{abs} on the temperature T is modeled:

$$k_{abs}(T) = aT^2 + bT + c.$$

Once the parameter vector $p = [a \;\; b \;\; c]'$ is determined, then the plant behaviour is completely described by the model introduced in Section 2. The parameter estimation problem, then, is that of retrieving the value of p based on measurements of properly chosen input/output signals. In our setup, we will consider a 10% step variation of the CO_2 inlet molar fraction as the input signal, while the temperature at point A as the output signal. All signals are sampled with sampling interval $\tau = 2s$. Note that the identification experiment is simple and can be easily reproduced by any user.

Table 1. The simulated data chart as the starting point of the two-stage method.

p_1	$D_1^N = \{y^1(1), u^1(1), \ldots, y^1(N), u^1(N)\}$
p_2	$D_2^N = \{y^2(1), u^2(1), \ldots, y^2(N), u^2(N)\}$
$\vdots$	$\vdots$
p_m	$D_m^N = \{y^m(1), u^m(1), \ldots, y^m(N), u^m(N)\}$

The parameter estimation is performed by the so-called Two-Stage (TS) method, Garatti and Bittanti (2013).

4.1 The TS Approach

An estimator for the problem at hand is just a function $\widehat{f}: \mathbb{R}^{2N} \to \mathbb{R}^3$ mapping the measured observations

$$\bar{D}^N = \{\bar{y}(1), \bar{u}(1), \bar{y}(2), \bar{u}(2), \ldots, \bar{y}(N), \bar{u}(N)\}$$

into the returned estimate:

$$\widehat{p} := \widehat{f}(\bar{y}(1), \bar{u}(1), \ldots, \bar{y}(N), \bar{u}(N)).$$

In standard approaches, like those based on Kalman filtering or Prediction Error Methods (PEM) in system identification (Ljung (1999); Söderström and Stoica (1989)), the map f is *implicitly* defined by means of some estimation criterion. This, however, poses some difficulties in using these approaches repeatedly, without human intervention, see Garatti and Bittanti (2013) for the details.

The TS approach develops along completely different ideas: it resorts to off-line intensive simulation runs in order to explicitly reconstruct a function $\widehat{f}: \mathbb{R}^{2N} \to \mathbb{R}^3$ mapping measured input/output data into a parameter estimate $\widehat{p}$.

To be precise, we use the *simulator* of the reactor to generate input/output data for a number of different values of the unknown parameter p chosen so as to densely cover a certain range of interest. That is, we collect N simulated measurements

$$D_1^N = \{y^1(1), u^1(1), \ldots, y^1(N), u^1(N)\}$$

for $p = p_1$; N simulated measurements

$$D_2^N = \{y^2(1), u^2(1), \ldots, y^2(N), u^2(N)\}$$

for $p = p_2$; and so forth and so on, so as to work out a set of, say m, pairs $\{p_i, D_i^N\}$, as summarized in Table 1.

Such set of data is referred to as the *simulated data chart*. From the simulated data chart, the function $\widehat{f}$ is reconstructed as that map minimizing the estimation error over simulated data, i.e.

$$\widehat{f} \leftarrow \min_{f \in \mathcal{F}} \frac{1}{m} \sum_{i=1}^{m} \left\| p_i - f(y^i(1), u^i(1), \ldots, y^i(N), u^i(N)) \right\|^2, \tag{3}$$

where $\mathcal{F}$ is a class of fitting functions. Should $\widehat{f}$ be found, then the true parameter vector corresponding to the actual

Table 2. The compressed artificial data chart.

p_1	$\widetilde{D}_1^n = \{\alpha_1^1, \ldots, \alpha_n^1\}$
p_2	$\widetilde{D}_2^n = \{\alpha_1^2, \ldots, \alpha_n^2\}$
$\vdots$	$\vdots$
p_m	$\widetilde{D}_m^n = \{\alpha_1^m, \ldots, \alpha_n^m\}$

measurements, say $\bar{D}^N = \{\bar{y}(1), \bar{u}(1), \ldots, \bar{y}(N), \bar{u}(N)\}$, can be estimated as

$$\widehat{p} = \widehat{f}(\bar{y}(1), \bar{u}(1), \ldots, \bar{y}(N), \bar{u}(N)).$$

Solving (3) is critical. In the TS approach, the resolution of (3) is split into two steps. This splitting is the key to obtain a good estimator $\widehat{f}$.

First stage. The first step consists of a compression of the information conveyed by input/output sequences D_i^N in order to obtain new data sequences $\widetilde{D}_i^n$ of reduced dimensionality. While in the data D_i^N the information on the unknown parameter p_i is scattered in a long sequence of N samples, in the new compressed artificial data $\widetilde{D}_i^n$ such information is contained in a short sequence of n samples ($n \ll N$). This leads to a new compressed artificial data chart composed of the pairs $\{p_i, \widetilde{D}_i^n\}$, $i = 1, \ldots, m$, see Table 2.

Each compressed artificial data sequence $\widetilde{D}_i^n$ is obtained by fitting a *simple black-box* model to each sequence $D_i^N = \{y^i(1), u^i(1), \ldots, y^i(N), u^i(N)\}$, and, then, by taking the parameters of this identified model, say $\alpha_1^i, \alpha_2^i, \ldots, \alpha_n^i$, as compressed artificial data, i.e. $\widetilde{D}_i^n = \{\alpha_1^i, \ldots, \alpha_n^i\}$.

Summing up, in the first stage a function $\widehat{g} : \mathbb{R}^{2N} \to \mathbb{R}^n$ is found, transforming each simulated data sequence D_i^N into a new sequence of compressed artificial data $\widetilde{D}_i^n$ still conveying the information on p_i. Function $\widehat{g}$ is defined by the chosen class of simple models used to fit simulated data along with the corresponding identification algorithm.

Second stage. Once the compressed artificial data chart has been worked out, problem (3) becomes that of finding a map $\widehat{h} : \mathbb{R}^n \to \mathbb{R}^q$ which fits the m compressed artificial observations into the corresponding parameter vectors, i.e.

$$\widehat{h} \leftarrow \min_{h \in \mathcal{H}} \frac{1}{m} \sum_{i=1}^{m} \left\| p_i - h(\alpha_1^i, \ldots, \alpha_n^i) \right\|^2, \qquad (4)$$

where $\mathcal{H}$ is a suitable function class.

Problem (4) is reminiscent of the original minimization problem in (3). However, being n small thanks to the compression of the information in the first stage, its resolution is not an issue anymore. One can e.g. resort to Neural Networks and solve (4) by means of the standard algorithms developed for fitting this class of nonlinear functions to the data.

Use of the two-stage method. After $\widehat{h}$ has been computed, the final estimator $\widehat{f}$ mapping input/output data into the parameter estimate $\widehat{p}$ is obtained as

$$\widehat{f} = \widehat{h} \circ \widehat{g} = \widehat{h}(\widehat{g}(\cdot)),$$

i.e. as the composition of $\widehat{g}$ and $\widehat{h}$.
Note that $\widehat{f}$ is constructed off-line, by means of simulation experiments only. However, when a real input/output sequence $\bar{D}^N = \{\bar{y}(1), \bar{u}(1), \ldots, \bar{y}(N), \bar{u}(N)\}$ is collected, the unknown parameter vector can be estimated as $\widehat{p} = \widehat{h}(\widehat{g}(\bar{D}^N))$, that is, by evaluating $\widehat{f}$ in correspondence of the actually seen data sequence. This evaluation can be easily performed by an automatic device, which can be used to generate estimates $\widehat{p}$ whenever it is needed, at very low computational cost and without any intervention of specialized personnel.

4.2 Application to the Reactor Model: Results

In order to apply the TS method to the reactor for CO_2 absorption/desorption, $m = 2500$ random values for $p = [a \ b \ c]'$ were extracted, ensuring that the corresponding k_{abs} were suitably bounded:

$$0.5\bar{k}_{abs}(T_i) \leq k_{abs}(T_i) \leq 2\bar{k}_{abs}(T_i), \quad i = 1, 2, 3,$$

where the $\bar{k}_{abs}(T_i)$'s were chosen as the result of the identification procedure discussed in Section 3: $\bar{k}_{abs}(T_1) = 5.8257 \times 10^{-8}$ m/s, $\bar{k}_{abs}(T_2) = 4.6707 \times 10^{-8}$ m/s and $\bar{k}_{abs}(T_3) = 4.6105 \times 10^{-8}$ m/s. Correspondingly, we ran 2500 simulations of the reactor, each time injecting a CO_2 molar fraction step of 10% as the input while the reactor was in steady-state condition and at an initial temperature $T = 60$ °C. Typical temperature outputs for different values of the parameter vector p are depicted in Fig. 5.

By sampling at 0.025 Hz the input and output signals, we obtained 2500 input/output sequences each $N = 150$ samples long:

$$u^i(1), y^i(1), u^i(2), y^i(2), \ldots, u^i(150), y^i(150),$$

$i = 1, 2, \ldots, 2500$. These sequences together with the 2500 extracted values for p formed the simulated data chart. As for the generation of the compressed artificial data chart, we noticed that, in our experiments, the output looks like an impulse response, because of the zero in the origin introduced by the external refrigerator, which forces the temperature to return to the initial value. Hence, by letting $\Delta u^i(t) = u^i(t) - u^i(t-1)$ be the impulse corresponding to the given step, we fitted to each generated data sequence a third-order state-space model

$$x(t+1) = Fx(t) + G\Delta u^i(t)$$
$$y^i(t) = Hx(t),$$

by using the Ho-Kalman algorithm, Ho and Kalman (1966). The parameters $\alpha_1^i, \alpha_2^i, \ldots, \alpha_{15}^i$, $i = 1, 2, \ldots, 2500$, were obtained as the entries of the identified matrixes F, G, H. The final estimator $\widehat{h}(\alpha_1^i, \alpha_2^i, \ldots, \alpha_{15}^i)$ was instead derived by resorting to a feed-forward 3-layers neural network, with 20 neurons in each hidden layer, Haykin (1998). The network weights were trained by the usual back-propagation algorithm. The order of the state-space model as well as that of the neural network were eventually chosen by means of cross-validation.

In order to test the TS estimator, we picked 500 new random values for the uncertain vector parameter p, and correspondingly we ran new 500 simulations of the reactor model in the same experimental conditions as in the training phase. The 500 data sequences obtained by sampling input and output signals at 0.025 Hz were made available to the TS estimator so as to generate 500 estimates of

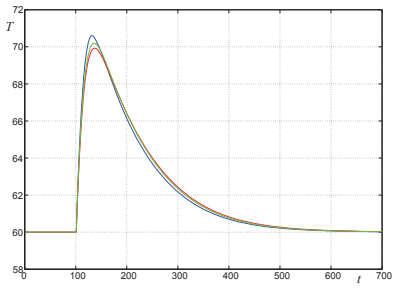

Fig. 5. Temperature at the reactor inlet while injecting an inlet CO_2 molar fraction step.

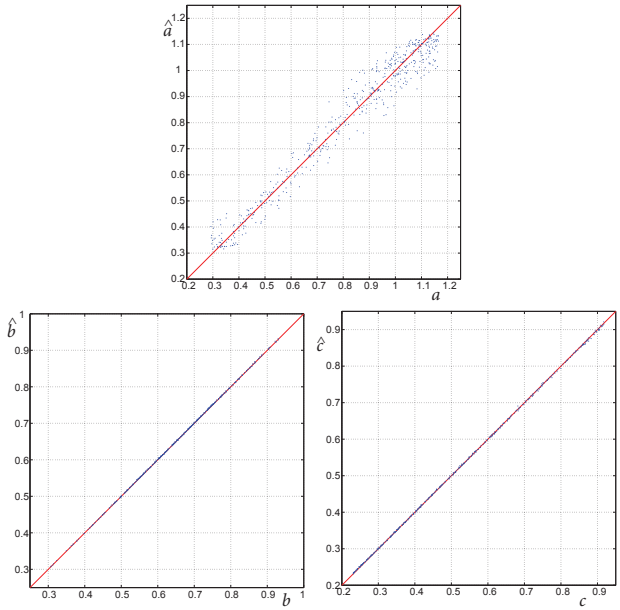

Fig. 6. Estimation results for parameters a, b, and c.

the parameter vector p. These estimates were eventually compared to the true values of the parameter vector so as to evaluate the performance of the obtained estimator (cross-validation). In Fig. 6, the estimates $\hat{a}$, $\hat{b}$, and $\hat{c}$, respectively, as returned by the TS estimator, are plotted against the true parameter values a, b, and c.

5. CONCLUSIONS

The dynamics of a recently introduced CO_2 capture process based on amines supported on solid pellets have been modelled, and a white-box TS technique has been applied to estimate the absorption and desorption kinetic parameters in the model. The method has proven a good estimation capability.

Activities have gone on with the design and realization of a four-reactor pilot plant, to treat 100 Nm^3/h feedgas flow rate,which has been installed and tested on a coal-fired conventional power station, owned by ENEL, in operation in Brindisi, in Italy. Tests on the plant in real operating conditions have shown that the sorbent has the same performance as in the laboratory scale reactor.

After the required scale-up to adequate its operating conditions to that pre-industrial plant, the model developed in this work will be employed to study the control problems related to coordination and synchronization of the reactors, in order to guarantee continuous operation and sorbent regeneration efficiency without spending too much energy in reactor heating and/or in pressure variation at reactor inlet or outlet (see, *e.g.*, Bittanti et al. (2012)). The TS method will be employed to generate suitable estimates of parameter vector p, and therefore of the kinetic parameters, whenever a tuning of the reactor model is needed along the reactors' life.

REFERENCES

Bittanti, S., Calloni, L., De Marco, A., Notaro, M., Prandoni, V., and Valsecchi, A. (2012). A process for CO_2 post combustion capture based on amine supported on solid pellets. In *Proceedings of the 8^{th} IFAC International Symposium on Advanced Control of Chemical Processes*. Furama Riverfront, Singapore.

Bittanti, S., Canevese, S., De Marco, A., Fenzi, L., Notaro, M., and Prandoni, V. (2010). Modelling and identification for carbon dioxide post combustion capture by amines supported on solid sorbents. In *Proceedings of the 9^{th} Annual Conference on Carbon Capture and Sequestration*. Pittsburgh, Pennsylvania, USA.

Ciferno, J.P., Ramezan, M., Skone, J., ya Nsakala, N., Liljedahl, G.N., Gearhart, L.E., Hestermann, R., and Rederstorff, B. (2007). Carbon dioxide capture from existing coal-fired power plants. Technical Report 401/110907, DOE/NETL Report. Available: http://www.netl.doe.gov/File Library/Research/Energy Analysis/Publications/CO2-Retrofit-From-Existing-Plants-Revised-November-2007.pdf.

De Marco, A., Fenzi, L., Notaro, M., and Canevese, S. (2010). CO_2 post-combustion capture by solid sorbents: Process model. Technical Report 10001332, RSE RdS Report. In Italian. Available: http://www.ricercadisistema.it.

Froment, G.F. and Bischoff, K.B. (1990). *Chemical Reactor Analysis and Design*. John Wiley & Sons, NY, USA.

Garatti, S. and Bittanti, S. (2013). A new paradigm for parameter estimation in system modeling. *International Journal of Adaptive Control and Signal Processing*, 27(8), 667–687.

Haykin, S. (1998). *Neural Networks: A Comprehensive Foundation*. Prentice Hall, Upper Saddle River, NJ, USA.

Ho, B.L. and Kalman, R.E. (1966). Effective construction of linear state-variable models from input/output functions. *Regelungstechnik*, 14(12), 545–592.

Krutka, H. and Sjostrom, S. (2011). Evaluation of solid sorbents as a retrofit technology for CO_2 capture from coal-fired power plants. Technical Report 05649FR01, DOE Report. Available: http://www.netl.doe.gov/File Library/Research/Coal/ewr/co2/evaluation-of-solid-sorbents-nov2011.pdf.

Ljung, L. (1999). *System Identification: Theory for the User*. Prentice-Hall, Upper Saddle River, NJ, USA.

Notaro, M. (2011). Post-combustion CO_2 capture by solid sorbents. In *Convegno nazionale AEIT 2011*. Milan, Italy. In Italian.

Notaro, M., Pardos Gotor, J.M., and Savoldelli, P. (2012). Method for capturing CO_2. WO Patent App. PCT/ES2012/070,137. Available: http://www.google.com/patents/WO2012120173A1?cl=en.

Notaro, M. and Pinacci, P. (2007). Carbon dioxide capture from flue gas by solid regenerable sorbents. In *Proceedings of the 3^{rd} International Conference on Clean Coal Technologies for our Future*. Cagliari, Italy.

Ruthven, D.M. (1984). *Principles of Adsorption and Adsorption Processes*. John Wiley & Sons, NY, USA.

Ruthven, D.M., Farooq, S., and Knaebel, K.S. (1994). *Pressure Swing Adsorption*. VCH, NY, USA.

Santacesaria, E., Morbidelli, M., Servida, A., Storti, G., and Carrà, S. (1982). Separation of xylenes on y zeolites. Note II: Breakthrough curves and their interpretation. *Industrial & Engineering Chemistry, Process Design and Development*, 21(3), 446–451.

Söderström, T. and Stoica, P. (1989). *System Identification*. Prentice-Hall, Englewood Cliffs, NJ, USA.